Preprints, 4th IFAC Conference on
Advances in Proportional-Integral-Derivative Control
Almería, Spain | June 12-14, 2024

On the hybrid MRAC-PID control: A comparison study ⋆

Juan D. Gil * **Igor M. L. Pataro** * **J. L. Guzmán** *
M. Berenguel *

* *Universidad de Almería, Centro Mixto CIESOL, ceia3, Ctra. Sacramento s/n, 04120, Almería, Spain (e-mail: juandiego.gil@ual.es. ilp428@inlumine.ual.es, joseluis.guzman@ual.es, beren@ual.es).*

Abstract:
This study performs a comparative analysis of three Model Reference Adaptive Control (MRAC) schemes grounded in Lyapunov theory. Specifically, it compares a pure MRAC controller with two hybrid MRAC-PID schemes, each integrating the PID component in a distinct manner within the control structure. The aim is to address a significant gap in the existing literature related to the lack of comparisons involving the different ways the MRAC and PID control can be hybridized. The developed controllers undergo extensive testing in simulated scenarios emphasizing model reference convergence and disturbance rejection. The results underscore that hybridizing the MRAC mechanism with a PID controller offers notable advantages in both performance and robustness, especially concerning disturbance rejection, a scenario in which the hybrid controllers improved by around 70 and 75 % the mean square error obtained with a pure MRAC controller. In general, these findings highlight the potential benefits of combining MRAC and PID techniques, providing insight into the improved control system performance that PID control can bring to conventional MRAC schemes.

Keywords: Adaptive control, PID control, hybrid control structure, process control.

1. INTRODUCTION

Model Reference Adaptive Control (MRAC) employs a closed-loop controller with adjustable parameters to optimize the system response and achieve a desired dynamic behavior in closed-loop. Specifically, in MRAC controllers, the adaptation mechanism dynamically modifies the controller parameters to align the process output with the output of the reference model. This model sets the expected (reference) output response that the system aims to track (Åström and Wittenmark, 2013). Thus, the use of MRAC controllers provides the advantage of accommodating system deviations from the reference response defined by the reference model, whether these deviations arise from uncertainties or disturbances (Shekhar and Sharma, 2018).

MRAC control finds prominent application in various domains, particularly in the control of robotic manipulators (Zhang and Wei, 2017), motor control (Humaidi et al., 2017; Nguyen et al., 2018), and diverse applications such as the stabilization of pendulum systems (Mendez et al., 2020). It should be noted that, in most cases, the MRAC mechanism is applied directly without including additional auxiliary control schemes to address robustness issues. However, an emerging trend involves hybridizing MRAC controllers with Proportional, Integral, and Derivative (PID) controllers, which provides potential advantages in terms of convergence, as discussed in detail by Zhang and Wei (2016). This hybridization strategy represents a nuanced approach that can potentially improve the adaptability and performance of MRAC controllers in various applications.

In the existing literature, some examples of the combination of PID and MRAC control can be found. Amrane and Chaiba (2015) proposed an MRAC-PID for a double-feed induction generator. The study conducted by Pawar and Parvat (2015) introduced an MRAC-PID controller for an inverted pendulum system; the integration of both control systems (i.e., MRAC and PID) was carried out to mitigate the limitations associated with traditional MRAC techniques. Zhou et al. (2016) designed an MRAC-PID controller for an inertial-stabilized aircraft platform focused on disturbance rejection. By and large, these examples collectively underscore the diverse applications and advantages sought through the combination of PID and MRAC methodologies, showcasing the benefits of such hybrid control systems in various domains. However, the main gap identified in the literature is the lack of consensus regarding the optimal approach to integrate the MRAC mechanism with a PID controller. Moreover, there is a dearth of comparisons involving the different ways in which MRAC and PID control can be hybridized. To the authors' knowledge, the only existing comparison is that proposed by Zhang and Wei (2016), which compared a pure MRAC

⋆ This work is a result of the CyberGreen Project, PID2021-122560OBI00, and the Agroconnect (www.agroconnect.es) facilities, grant EQC2019-006658-P, both funded by MCIN/AEI/10.13039/501100011033 and by ERDF A way to make Europe. Igor M. L. Pataro acknowledges the financial support of the National Council for Scientific and Technological Development (CNPq, Brazil) under grant 201143/2019 − 4.

scheme with a hybrid MRAC-PID controller in terms of convergence. However, in that work, only a hybrid scheme is employed, in which the MRAC mechanism adjusts the control signal of the PID controller.

On the basis of the above literature review, this paper conducts a comparative analysis of three MRAC schemes developed following the Lyapunov theory. It specifically compares a pure MRAC controller with two hybrid MRAC-PID schemes, each integrating the PID component in a different manner within the control structure. Particularly, in the first hybrid controller, the MRAC mechanism is responsible for adjusting the reference of the PID control loop. On the contrary, in the second hybrid controller, the MRAC mechanism adjusts the PID control signal. The design of both approaches is developed following the principles outlined by Åström and Wittenmark (2013) regarding the Lyapunov theory. Moreover, the corresponding block diagrams are fully depicted, allowing for practical implementation. Finally, the controllers are compared through simulations, utilizing two distinct scenarios focused on model reference convergence and disturbance rejection.

The paper is structured as follows: Section 2 is dedicated to the design of the different controllers. Section 3 presents and analyzes the main results derived from the application of the developed controllers in the proposed simulation scenarios. Lastly, Section 4 outlines the key conclusions drawn and offers recommendations for future research.

2. CONTROLLERS' DESIGN

In this section, MRAC-based control solutions are developed for the simplest case: a first-order system without time delay. First, the MRAC mechanism based on the Lyapunov theory is depicted. Afterward, two hybrid MRAC-PID control structures based on the same principles are proposed.

2.1 MRAC based on the Lyapunov theory

Take into account the first-order system defined by the equation:

$$\frac{dy(t)}{dt} = -a_1 \cdot y(t) + a_2 \cdot u(t), \tag{1}$$

where $u(t)$ represents the input to the process, $y(t)$ is the observable output of the process, and a_1 and a_2 are the unknown parameters of the process.

Now, consider the desired dynamics in closed-loop as expressed by the equation:

$$\frac{dy_m(t)}{dt} = -a_{1,m} \cdot y_m(t) + a_{2,m} \cdot u_c(t), \tag{2}$$

where $y_m(t)$ signifies the desired closed-loop response, $a_{1,m}$ and $a_{2,m}$ are predetermined gains, and $u_c(t)$ represents the command signal intended as a reference.

Let now introduce an adaptive control law to integrate the adaptation mechanism as follows:

$$u(t) = \theta_1(t) \cdot u_c(t) - \theta_2(t) \cdot y(t). \tag{3}$$

At this point, let define the error between the actual process output and the desired behavior as:

$$e_m(t) = y(t) - y_m(t), \tag{4}$$

Given that the main objective of the proposed controller is to minimize this error, it is logical to formulate a corresponding differential equation. Using Eqs. (1), (2), and (3) yields the following result:

$$\frac{de_m(t)}{dt} = -a_{1,m} \cdot e_m(t) - (a_2 \cdot \theta_2(t) + a_1 - a_{1,m}) \cdot y(t) + (a_2 \cdot \theta_1(t) - a_{2,m}) \cdot u_c(t). \tag{5}$$

It should be noted that the error goes to zero if the adaptable parameters (that is, θ_1 and θ_2) reach the following equilibrium values:

$$\overline{\theta_1} = \frac{a_{2,m}}{a_2}, \quad \overline{\theta_2} = \frac{a_{1,m} - a_1}{a_2}. \tag{6}$$

To create a mechanism to adjust the parameters θ_1 and θ_2 to the previous values, assume a constant term given by $a_2\gamma$ such that $a_2\gamma > 0$ and introduce the following Lyapunov function (time dependence has been omitted for the sake of clarity) according to the ideas presented by Åström and Wittenmark (2013):

$$V(e_m, \theta_1, \theta_2) = \frac{1}{2} \cdot \Big[e_m^2 + \frac{1}{a_2\gamma} \cdot (a_2 \cdot \theta_2 + a_1 - a_{1,m})^2 + \frac{1}{a_2\gamma} \cdot (a_2 \cdot \theta_1 - a_{2,m})^2\Big]. \tag{7}$$

Note that Eq. (7) is differentiated with respect to time, thus allowing one to determine its Lyapunov stability:

$$\frac{dV}{dt} = e_m \cdot \frac{de_m}{dt} + \frac{1}{\gamma} \cdot (a_2 \cdot \theta_2 + a_1 - a_{1,m}) \cdot \frac{d\theta_2}{dt} + \frac{1}{b\gamma} \cdot (a_2 \cdot \theta_1 - a_{2,m}) \cdot \frac{d\theta_1}{dt}. \tag{8}$$

Thus, by introducing Eq. (4), the previous equation becomes:

$$\frac{dV}{dt} = -a_{1,m} \cdot e_m^2 + \frac{1}{\gamma} \cdot (a_2 \cdot \theta_2 + a_1 - a_{1,m}) \cdot (\frac{d\theta_2}{dt} - \gamma \cdot y \cdot e_m) + \frac{1}{\gamma} \cdot (a_2 \cdot \theta_1 - a_{2,m}) \cdot (\frac{d\theta_1}{dt} + \gamma \cdot u_c \cdot e_m), \tag{9}$$

so that if the adaptive parameters are updated as:

$$\frac{d\theta_1}{dt} = -\gamma \cdot u_c \cdot e_m, \quad \frac{d\theta_2}{dt} = \gamma \cdot y \cdot e_m, \tag{10}$$

Eq. (9) results in:

$$\frac{dV}{dt} = -a_{1,m} \cdot e_m^2. \tag{11}$$

Since it is negative semidefinite, it is Lyapunov stable (notice that $a_{1,m}$ must be positive for the closed-loop system to be stable). Furthermore, the boundedness and convergence of Eq. (11) can be proven if it is locally Lipschitz (Åström and Wittenmark, 2013). Therefore, by differentiating the equation with respect to time, we get the following:

$$\frac{d^2V}{dt^2} = -2 \cdot a_{1,m} \cdot e_m \cdot \frac{de_m}{dt}. \tag{12}$$

Now, if Eq. (4) is substituted, it is evident that $\frac{d^2V}{dt^2}$ is a function of e_m, y, and u_c, which are bounded signals. This implies that $\frac{d^2V}{dt^2}$ is bounded and $\frac{dV}{dt}$ is continuous, so the system is Lyapunov stable and locally Lipschitz. More details on this issue can be found in (Åström and Wittenmark, 2013).

The MRAC controller can now be displayed using the previous development, as shown in Fig. 1. In this scheme, Eq. (1) is included in the block *System*, whereas Eq. (2) is reflected in the block *Reference model*.

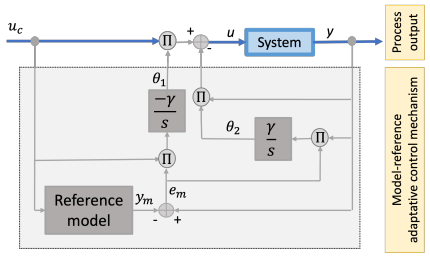

Fig. 1. Schematic diagram of the pure MRAC controller.

2.2 Hydrid MRAC-PID: Solution 1

One of the primary limitations of an MRAC structure is its relatively weak robustness capability compared to other control structures (Vargas-Martínez et al., 2015). To address this limitation, a conventional PID controller can be incorporated into the MRAC control loop, resulting in a hybrid MRAC-PID control solution. This approach enables us to exploit the power and robustness of PID controllers within an MRAC mechanism.

In fact, one of the most straightforward methods of integrating the PID and MRAC strategies involves substituting the *system* block from the preceding section (see Fig. 1), with a PID-based feedback control loop, as shown in Fig. 2. Note that in this case, the development shown in the previous section is the same, the only difference is that Eq. (1) reflects closed-loop system dynamics instead of the open-loop ones. Thus, in this case, the MRAC mechanism is responsible for adjusting the setpoint of the PID feedback control loop in order to obtain the desired dynamics imposed by the reference model.

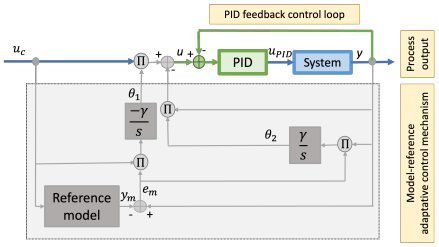

Fig. 2. Schematic diagram of the hybrid MRAC-PID controller, solution 1.

2.3 Hydrid MRAC-PID: Solution 2

As mentioned in the scheme outlined in the preceding section, the MRAC mechanism adjusts the reference of the PID control loop. An alternative approach to hybridize MRAC and PID involves the MRAC mechanism directly modifying the control signal computed by the PID controller, following the ideas presented by Khan and Swamy (2016). For this case, consider Eqs. (1) and (2) and the following adaptive control law:

$$u(t) = \theta_1(t) \cdot u_{PID}(t) - \theta_2(t) \cdot y(t). \tag{13}$$

where:

$$u_{PID}(t) = K_p \cdot \left[1 + \frac{1}{T_i} \cdot g + T_d \cdot p\right] \cdot e_{PID}(t), \tag{14}$$

where p and g have been introduced as the operators $\frac{d}{dt}$ and $\int_{\zeta=0}^{t} d\zeta$, respectively, K_p is the proportional gain, T_i the integral time, and T_d is the derivative time of the PID controller. Moreover, the PID error equation is given by:

$$e_{PID}(t) = u_c(t) - y(t). \tag{15}$$

Note that the model reference error is defined as in Eq. (4).

As pointed out in Section 2.1, the objective is to minimize the error in Eq. (4) so that the differential equation in this case can be formulated as:

$$\frac{de_m(t)}{dt} = -a_{1,m} \cdot e_m(t) - (a_2 \cdot \theta_2(t) + a_1 - a_{1,m}) \cdot y(t) + a_2 \cdot \theta_1(t) \cdot u_{PID}(t) - a_{2,m} \cdot u_c(t). \tag{16}$$

By incorporating now Eq. (15) and adding and subtracting u_{PID} on the right-hand side, the previous equation becomes (note that the dependence with time has been omitted for the sake of clarity):

$$\frac{de_m}{dt} = -a_{1,m} \cdot e_m - a_{2,m} \cdot e_{PID} - (a_2 \cdot \theta_2 + a_{2,m} + a_1 - a_{1,m}) \cdot y + (a_2 \cdot \theta_1 + 1) \cdot u_{PID} - u_{PID}. \tag{17}$$

As can be observed, in this case, the error will go to zero if the adaptive parameters converge to the following values:

$$\overline{\theta_1} = \frac{-1}{a_2}, \quad \overline{\theta_2} = \frac{a_{1,m} - a_1 - a_{2,m}}{a_2}. \tag{18}$$

It is also important to mention that the error in this case does not depend only on the e_m-term, but the error of the feedback control loop (i.e., e_{PID}) is also involved, as it appears directly in Eq. (17) and through the term u_{PID} as defined in Eq. (14). Thus, it becomes evident that achieving convergence between the model and the desired behavior requires a zero PID error signal (e_{PID}). Since $e_{PID}(t) = u_c(t) - y(t)$ and $e_m(t) = y(t) - y_m(t)$, at the convergence point, the system output (y) must be equal to both the command signal (u_c) and the desired output (y_m). This condition is achievable only if, considering first-order reference models, they maintain unity gain, that is, $a_{1,m} = a_{2,m}$ in Eq. (2), which is typically imposed in process control for tracking control problems. Note that, by doing this, at the convergence point, $u_c(t) = y_m(t) = y(t)$. This is an important remark that must be taken into account for the application of this hybrid controller.

At this point, let define a Lyapunov function following the principles outlined in Section 2.1 as follows:

$$V(e_m, \theta_1, \theta_2) = \frac{1}{2} \cdot \left[e_m^2 + \frac{1}{a_2\gamma} \cdot (a_2 \cdot \theta_2 + a_{2,m} + a_1 - a_{1,m})^2 + \frac{1}{a_2\gamma} \cdot (a_2 \cdot \theta_1 + 1)^2\right]. \tag{19}$$

By differentiating the previous equation with respect to time and incorporating Eq. (17) we obtain:

$$\frac{dV}{dt} = -a_{1,m} \cdot e_m^2 - a_{2,m} \cdot e_m \cdot e_{PID} + \frac{1}{\gamma} \cdot (a_2 \cdot \theta_2 + a_{2,m} + a_1 - a_{1,m}) \cdot \left(\frac{d\theta_2}{dt} - \gamma \cdot y \cdot e_m\right) + \frac{1}{\gamma} \cdot (a_2 \cdot \theta_1 + 1) \cdot \left(\frac{d\theta_1}{dt} + \gamma \cdot u_{PID} \cdot e_m\right) - u_{PID} \cdot e_m, \tag{20}$$

so that if the adaptive parameters are updated as:

$$\frac{d\theta_1}{dt} = -\gamma \cdot u_{PID} \cdot e_m, \quad \frac{d\theta_2}{dt} = \gamma \cdot y \cdot e_m, \tag{21}$$

the following equation is derived:

$$\frac{dV}{dt} = -a_{1,m} \cdot e_m^2 - a_{2,m} \cdot e_m \cdot e_{PID} - u_{PID} \cdot e_m, \tag{22}$$

which, again, is a negative semi-definite and, therefore, Lyapunov stable. Note that the previous equation is negative semi-definite since i) it contains the term e_m^2 in the first term, ii) in the second, it has the multiplication of $e_m \cdot e_{PID}$, which are errors with the same sign, since Eq. (2) must have a unity gain, and iii) it contains the term $u_{PID} \cdot e_m$ in the third term. In this case, please take into account the definition in Eq. (14), so that the third term in Eq. (22) can be written as $K_p \cdot \left[1 + \frac{1}{T_i} \cdot g + T_d \cdot p\right] \cdot e_{PID} \cdot e_m$, which, again, is a multiplication between the error signals.

Now, as in Section 2.1, the boundedness and convergence can be proven if it is locally Lipschit. Consequently, by differentiating the equation with respect to time, we obtain the following

$$\frac{d^2V}{dt^2} = -2 \cdot a_{1,m} \cdot e_m \cdot \frac{de_m}{dt} - (u_{PID} \cdot \frac{de_m}{dt} + e_m \cdot \frac{du_{PID}}{dt}) - a_{2,m} \cdot (e_m \cdot \frac{de_{PID}}{dt} + e_{PID} \cdot \frac{de_m}{dt}). \tag{23}$$

Again, $\frac{d^2V}{dt^2}$ is bounded, and $\frac{dV}{dt}$ is continuous, so the system is Lyapunov stable and locally Lipschitz.

The schematic diagram of the MRAC controller can now be depicted in accordance with the previous development, as illustrated in Fig. 3. As in Section 2.1, in this scheme, Eq. (1) is included in the block *System*, whereas Eq. (2) is reflected in the block *Reference model*.

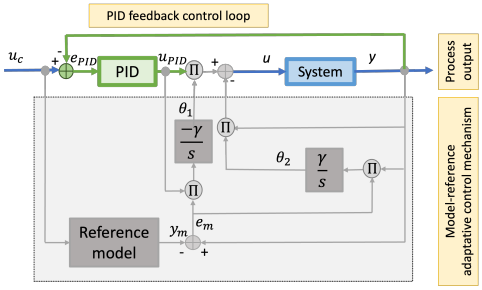

Fig. 3. Schematic diagram of the hybrid MRAC-PID controller, solution 2.

3. RESULTS

This section shows the results obtained with the different control configurations, that is, i) MRAC, ii) Hybrid MRAC-PID, solution 1, iii) Hybrid MRAC-PID, solution 2. The controllers were tested in two distinct scenarios, focusing on model reference convergence and disturbance rejection. For the different tests, the system in Eq. (1) was considered as $a_1 = 0.5$ and $a_2 = 1$, while the desired behavior in Eq. (2) as $a_{1,m} = 2$ and $a_{2,m} = 2$. Furthermore, the PID controller was configured only with proportional and integral terms following the pole-zero cancelation method (Åström and Hägglund, 2006). The closed-loop time constant was set to be 0.6 times faster than the open-loop dynamics, resulting in $K_p = 0.833$ [-] and $T_i = 1$ s. It is important to note that the configuration employed for the PID equation adhered to the ideal form. With respect to the tuning of the γ-parameter, this will be discussed in the following section.

3.1 Model reference adjustment and convergence

The initial simulation experiment assessed the convergence of the different control structures to the reference model. To achieve this, the reference signal u_c was set as a square wave with an amplitude of 2 and a frequency of 0.001 Hz. Furthermore, three different γ-values (0.001, 0.01, and 0.1) were examined for each controller to analyze the impact of this parameter on the controller performance. The results obtained are presented in Fig. 4.

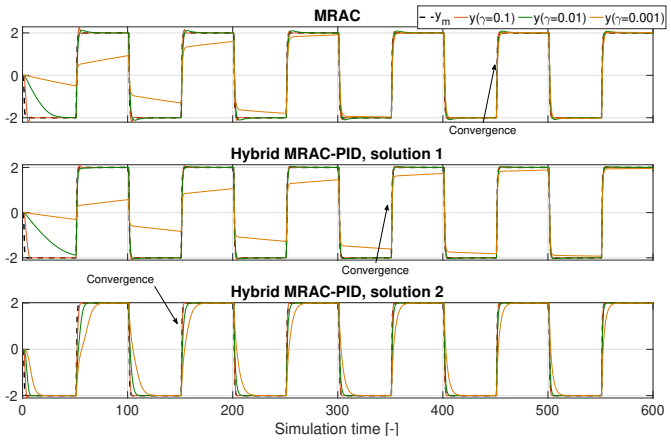

Fig. 4. Outputs of the controller with the different γ-values. Note that y_m is the output of the reference model, while the rest of the signals are the output with the different γ values for each configuration.

It is worth noting that Fig. 4 exclusively displays the system output, a choice made to enhance the clarity of result visualization with varying γ-values. The examination of the control signal behavior and a detailed analysis of adaptive parameters (θ_1 and θ_2) will be thoroughly discussed in the subsequent section. However, the moment in which the adaptive parameters (θ_1 and θ_2) reached convergence for the best γ-value configuration for each case is marked in the figure.

As can be seen, in general, low γ-values led to slow convergence in all cases, with special relevance in the MRAC and Hybrid MRAC-PID, solution 1. This is because in these configurations, the adjustment mechanism has an important weight in the controller performance since, in the first, it directly computes the control signal, and in the second, it is responsible for modifying the reference of the PID control loop. In the case of Hybrid MRAC-PID solution 2, the configuration of the control scheme gives certain advantages since, as can be seen in Eq. (16), the PID controller is also involved in the adjustment to the reference model, so the convergence was faster for all the γ-values. It should also be noted that although higher values of γ provided a faster adjustment, overshoots were observed in MRAC and hybrid MRAC-PID, solution 1, which must be considered in practical implementations.

To quantitatively observe the advantages of each controller in terms of adjustment, Tab. 1 presents the Mean Square Error (MSE) of each controller with different γ-values with respect to the reference model. As can be seen, in all cases, the smallest MSE value was obtained with $\gamma = 0.1$, and, in particular, the lowest value was provided by the Hybrid MRAC-PID configuration, solution 2, with an MSE of 0.0043. Another aspect to highlight is that the MRAC scheme provided a smaller MSE value than Hybrid MRAC-PID, solution 1, so the inclusion of the PID following that scheme did not provide advantages in terms of adjustment, although it does provide other types of advantages as will be shown in the next section.

Table 1. MSE of the different control configurations with the different γ-values with respect to the reference model.

	γ =0.1	γ =0.01	γ =0.001
MRAC	0.0050	0.0407	0.3104
Hybrid MRAC-PID, solution 1	0.0055	0.0527	0.5033
Hybrid MRAC-PID, solution 2	0.0043	0.0401	0.2799

3.2 Disturbance rejection

In the second test, the aim was to assess the performance and robustness of the controllers in the presence of disturbances. Thus, the reference signal (i.e., u_c) was maintained as in the previous section. However, a disturbance was introduced into the process output at simulation time 575, as illustrated in Fig. 5. Note that this disturbance consisted of a step of 1 plus band-limited white noise, with a noise power of 5 and a sample time of 60. The results obtained in this test are presented in Figs. 6, 7, and 8 for the MRAC, hybrid MRAC-PID solution 1, and hybrid MRAC-PID solution 2, respectively.

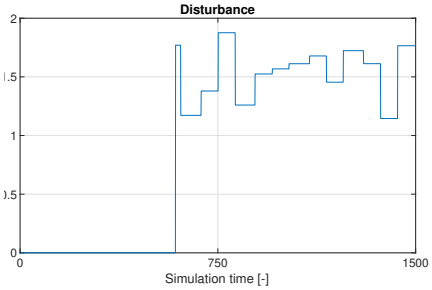

Fig. 5. Disturbance signal used as a reference in the simulation test.

As can be seen, until the moment when the disturbance was introduced (see the mark in Figs. 6-(1), 7-(1), and 8-(1)), all controllers almost reached convergence in the adaptation parameters (θ_1 and θ_2), see Figs. 6-(3), 7-(3), and 8-(3), observing the same results and trends as those discussed in the previous section. The main differences between the controllers can be seen in the rejection of the disturbance. In general, the two solutions that incorporate a PID controller (Figs. 7 and 8) exhibited faster rejection of disturbances. This was attributed to the PID controller operating on a faster time scale compared to the MRAC mechanism, allowing for a quicker response to reject disturbances. This fact also produced an extra advantage, which was that the convergence of the adaptation parameters was hardly altered in both cases, see Figs. 7-(3) and 8-(3).

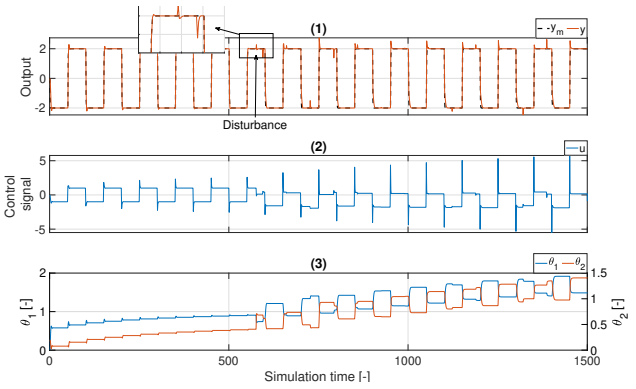

Fig. 6. MRAC control system performance during simulation. All the signals are according to the scheme depicted in Fig. 1.

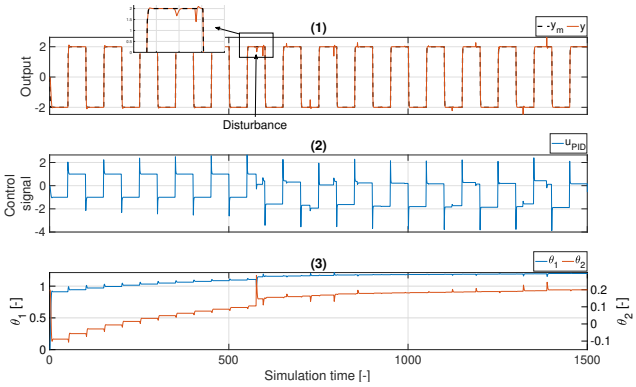

Fig. 7. Hybrid MRAC-PID controller, solution 1. All the signals are according to the scheme depicted in Fig. 2.

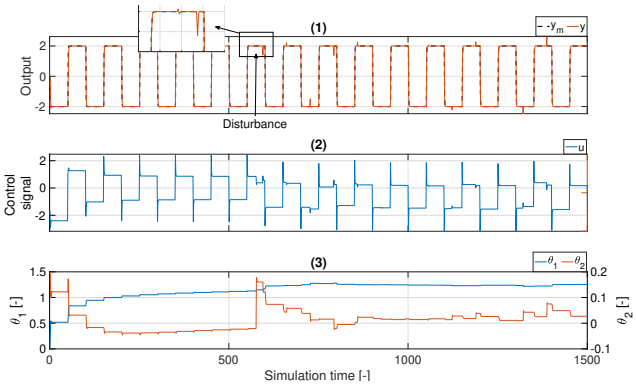

Fig. 8. Hybrid MRAC-PID controller, solution 2. All the signals are according to the scheme depicted in Fig. 3.

In the case of the MRAC controller (see Fig. 6), it can be seen how it also managed to reject the disturbance, even though it did not include a PID mechanism and its control action lies purely in the integrators of the adaptation law. However, it can be seen that the convergence of the adaptation parameters was completely altered (see Fig. 6)-(3)). This was quite significant since the parameters' values showed an upward and oscillating trend, which translated into increasingly aggressive control actions (see Fig. 6)-(2)). It should be noted that the test was stopped at instant 1500 for improved visualization. However, this trend persisted over time, leading to progressively more aggressive control actions. Consequently,

in practical implementations, particularly for systems with input constraints, applying such aggressive controls could be impossible or pose significant challenges. In addition, this behavior indicated instability, which is one of the problems stated by Åström and Wittenmark (2013) when a pure MRAC controller is subjected to large amplitude changes either in the reference or caused by disturbances, as in this case.

Finally, Tab. 2 shows the MSE of each of the controllers with respect to the reference model, as well as the Control Effort Total Variation (CETV), which respresents the sum of the absolute values of the increments of the control signal. As observed, the magnitude of MSE obtained by the schemes that incorporate PID is significantly lower, improving by around 70 and 75 % the performance of the MRAC controller for hybrid MRAC-PID solution 1 and solution 2, respectively.

Table 2. MSE of the different control configurations with respect to the reference model.

	MSE	CETV
MRAC	0.0188	228.13
Hybrid MRAC-PID, solution 1	0.0058	171.02
Hybrid MRAC-PID, solution 2	0.0044	153.35

4. CONCLUSION

This paper provides a comparative analysis of three MRAC schemes grounded in the Lyapunov theory. Specifically, it contrasts a pure MRAC controller with two hybrid MRAC-PID schemes, each incorporating the PID component in a distinct manner within the control structure. The controllers were tested in two different scenarios focused on model reference convergence and disturbance rejection. The results obtained allow us to draw the following conclusions:

- All controllers demonstrated satisfactory adjustment to the reference model. In particular, the proposed hybrid MRAC-PID solution 2 (with the MRAC mechanism adjusting the control signal of the PID controller) exhibited improved MSE values, underscoring the advantages of incorporating a PID into the adaptation mechanism according to this specific scheme for the adjustment of the reference model.
- Regarding disturbance rejection, the schemes incorporating PID exhibited markedly superior performance. This can be attributed to the PID mechanism operating on a faster time scale compared to the MRAC one. Thus, the hybrid MRAC-PID solution 1 and solution 2 improved by around 70 and 75 % the MSE performance of the MRAC controller, respectively. Moreover, the inclusion of the PID played a fundamental role in the robustness of the MRAC controller facing large amplitude changes caused by disturbances.

In general, the findings of this work underscore the potential advantages of integrating MRAC and PID techniques, providing insights on the improved performance of the control system that PID control can bring to traditional MRAC schemes.

Future work will be aimed at analyzing the performance of the different control schemes for systems of higher orders and/or time delay with input constraints and obtaining practical rules for tuning the γ-parameter.

REFERENCES

Amrane, F. and Chaiba, A. (2015). Comparative study on the performance of Fuzzy-PID and MRAC-PID controllers based on DPC with SVM for DFIG using MPPT strategy. In *International Conference on Automatic control, Telecommunications and Signals (ICATS15)*, 1–6.

Åström, K.J. and Wittenmark, B. (2013). *Adaptive control*. Courier Corporation.

Åström, K.J. and Hägglund, T. (2006). *Advanced PID control*. ISA-The Instrumentation, Systems and Automation Society.

Humaidi, A.J., Hameed, A.H., and Hameed, M.R. (2017). Robust adaptive speed control for DC motor using novel weighted E-modified MRAC. In *2017 IEEE International Conference on Power, Control, Signals and Instrumentation Engineering (ICPCSI)*, 313–319. IEEE.

Khan, A. and Swamy, M.S. (2016). Modified MRAC based on Lyapunov theory for improved controller efficiency. In *2016 International Conference on Automatic Control and Dynamic Optimization Techniques (ICACDOT)*, 989–995. IEEE.

Mendez, E., Baltazar-Reyes, G., Macias, I., Vargas-Martinez, A., de Jesus Lozoya-Santos, J., Ramirez-Mendoza, R., Morales-Menendez, R., and Molina, A. (2020). ANN based MRAC-PID controller implementation for a Furuta pendulum system stabilization. *Advances in Science, Technology and Engineering Systems Journal*, 5(3), 324–333.

Nguyen, A.T., Rafaq, M.S., Choi, H.H., and Jung, J.W. (2018). A model reference adaptive control based speed controller for a surface-mounted permanent magnet synchronous motor drive. *IEEE Transactions on Industrial Electronics*, 65(12), 9399–9409.

Pawar, R. and Parvat, B. (2015). Design and implementation of MRAC and modified MRAC technique for inverted pendulum. In *2015 International Conference on Pervasive Computing (ICPC)*, 1–6. IEEE.

Shekhar, A. and Sharma, A. (2018). Review of model reference adaptive control. In *2018 International Conference on Information, Communication, Engineering and Technology (ICICET)*, 1–5. IEEE.

Vargas-Martínez, A., Minchala Avila, L.I., Zhang, Y., Garza-Castañón, L.E., and Badihi, H. (2015). Hybrid adaptive fault-tolerant control algorithms for voltage and frequency regulation of an islanded microgrid. *International Transactions on Electrical Energy Systems*, 25(5), 827–844.

Zhang, D. and Wei, B. (2016). Convergence performance comparisons of PID, MRAC, and PID+MRAC hybrid controller. *Frontiers of Mechanical Engineering*, 11, 213–217.

Zhang, D. and Wei, B. (2017). A review on model reference adaptive control of robotic manipulators. *Annual Reviews in Control*, 43, 188–198.

Zhou, X., Yang, C., Cai, T., et al. (2016). A model reference adaptive control/PID compound scheme on disturbance rejection for an aerial inertially stabilized platform. *Journal of Sensors*, 2016.